

THE 4TH INTERNATIONAL CONFERENCE ON ALUMINUM ALLOYS

DEVELOPMENT OF RECRYSTALLIZATION TEXTURES IN THE ALLOY Al-1.3%Mn IN THE PRESENCE OF PARTICLES

O. Engler, P. Yang, G. Gottstein

Institut für Metallkunde und Metallphysik, RWTH Aachen, D-52056-Aachen, Germany

Abstract

The development of the recrystallization texture in high purity Al-1.3%Mn containing large Al₆Mn-precipitates was investigated by means of X-ray macrotecture analysis, supplemented by local orientation measurement by electron diffraction in a SEM (EBSD) and in a TEM (CBED). A combination of these three techniques for orientation determination with increasing spatial resolution yielded a more comprehensive information about the underlying recrystallization mechanisms than possible by using only one of these techniques.

The recrystallization texture develops from a competition between the Cube-texture and particle stimulated nucleation (PSN). These effects are discussed in terms of the formation and the subsequent growth behaviour of the recrystallization nuclei.

Introduction

It is well established now that particle stimulated nucleation (PSN) in Al-alloys containing large second phase particles ($>1\mu\text{m}$) as *e.g.* in Al-Mn 3xxx alloys generally leads to a weakening of the recrystallization texture, in particular, of the Cube-orientation $\{001\}\langle 100\rangle$ (*e.g.* [1-5]). In the current study texture evolution during recrystallization nucleation and subsequent growth in high purity Al-1.3%Mn containing Al₆Mn-precipitates was analysed. Besides X-ray macrotecture analysis, local orientation measurements by electron diffraction in a SEM (EBSD) and in a TEM (CBED) were performed in order to gain conclusions about the contribution of the various nucleation events to the resulting recrystallization texture.

Experimental Methods and Characterization of the Starting Material

A sample was prepared from high purity Al with 1.3 wt% (0.64 at%) Mn and pre-treated in such a way that it was fully recrystallized (initial grain size $\sim 40\mu\text{m}$) and contained a volume fraction of 3.6% homogeneously dispersed Al₆Mn-particles with a mean size of 2-3 μm . This sample was cold rolled to various reduction degrees up to 97.5%. Subsequently, the sheets were exposed to isothermal recrystallization treatments for various times at 350°C in a salt bath. Details of sample preparation as well as results about further studies regarding different deformation degrees, annealing temperatures and precipitation states will be given elsewhere [6]. X-ray macrotectures were examined after complete recrystallization by computation of the ODFs from four incomplete pole figures according to the series expansion method [7]. The data were ghost corrected by using Gauss-type scattering functions [8].

For TEM investigations longitudinal sections were prepared from the 80% rolled sheet after annealing for 30s at 350°C. At this annealing stage less than 1% of the entire volume was recrystallized, so that the nucleation sites of first recrystallized grains could easily be distinguished from each other. The slices were mechanically polished down to 70-100µm, and TEM-foils were produced by conventional twin-jet polishing (Tenupol). The orientations of the recrystallization nuclei and the new grains were determined from Kikuchi lines in the diffraction pattern. For improvement of spatial resolution a convergent beam was used. This procedure will be referred to as Convergent Beam Electron Diffraction (CBED) in the following. A JEOL EX2000 operating at 200kV was utilized for these measurements.

In order to study the development of the recrystallization texture in more detail, microtextures were determined in several samples at a partially recrystallized stage by means of Electron Back Scatter Diffraction (EBSD) in a SEM [9]. For a statistical evaluation of the resulting data ODFs were computed by associating each single grain orientation with a Gauss type scattering peak (half width 6°) in the Euler angle space.

Results

Recrystallized State

After complete recrystallization all samples exhibited a microstructure composed of small equiaxed grains. Fig.1 shows the resulting recrystallization texture in terms of the ODF of a 92% rolled sheet. The texture comprised a quite strong Cube orientation $\{001\}\langle 100\rangle$ with considerable scatter about RD and ND. Furthermore, at deformation degrees exceeding 90% the so called P-orientation $\{011\}\langle 122\rangle$ [at $(64^\circ, 45^\circ, 0^\circ)$] was observed, which slightly sharpened with progressing deformation. (As most interesting textural features are visible in the $\varphi_2=0^\circ$ -section of the ODFs (Fig.1), in the following the texture representation will be confined to this section.)

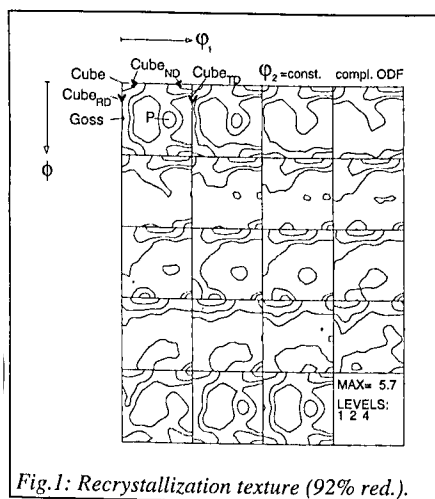


Fig.1: Recrystallization texture (92% red.).

Nucleation Sites

Microstructure investigations of the sheet rolled to 80% reduction in the TEM proved that two different nucleation sites of recrystallization were active.

(i) Cube-bands (Fig.2): During the anneal some subgrains within these Cube-bands grew and finally few of them were able to grow outside the band to consume the deformed matrix. The local orientations of several of the subgrains were determined by CBED (corresponding sites visible by the contamination spots in Fig.2). A typical result is shown in Fig.3. The bands exhibited Cube-orientations which were significantly shifted either around RD or, in fewer cases, around TD. In contrast, (sub)grains with an exact Cube-orientation (say within 5°), were not detected. For the new grains finally growing from the Cube-bands into the deformed matrix a very similar orientation distribution was found, as apparent from the corresponding ODF (Fig.4).

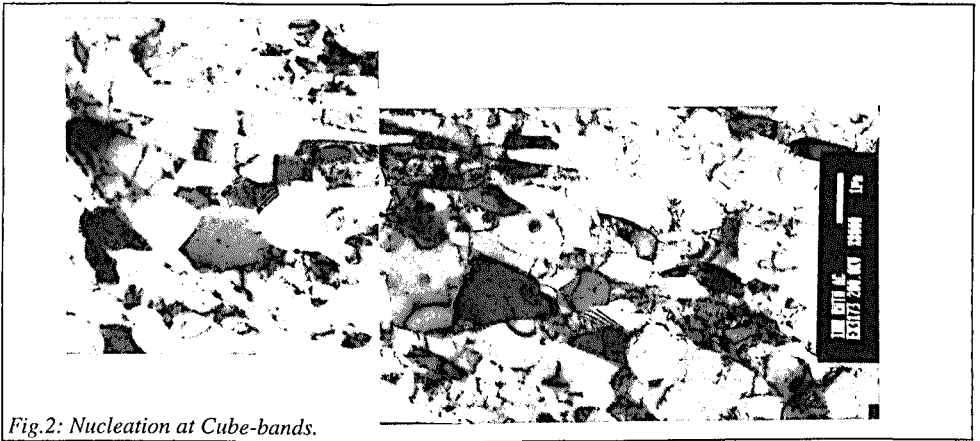


Fig.2: Nucleation at Cube-bands.

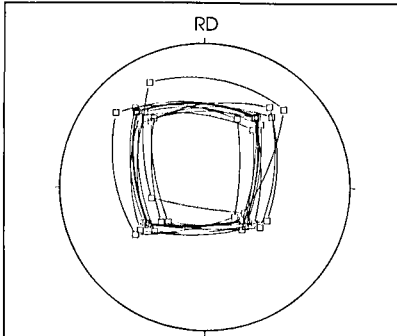


Fig.3: Orientation of subgrains in Fig.2.

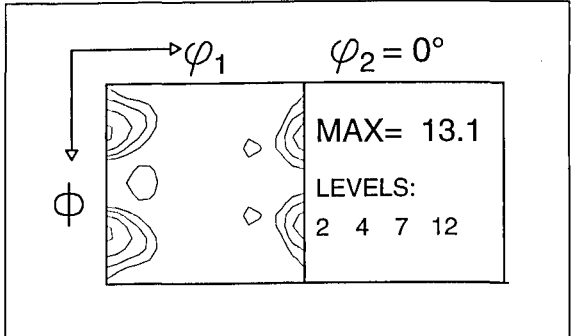


Fig.4: ODF of CBED-results of new grains in Cube-bands.

(ii) PSN (Fig.5): Additionally, nucleation from deformation zones around the Al_6Mn -particles was observed. Whereas the microstructure of the matrix was characterized by (recovered) microbands, very fine subgrains formed in the deformation zones around the particles (Fig.5), apparently due to the interaction between particles and dislocations. During annealing, one or a few of these subgrains finally were able to grow into the surrounding deformed matrix (Fig.5).

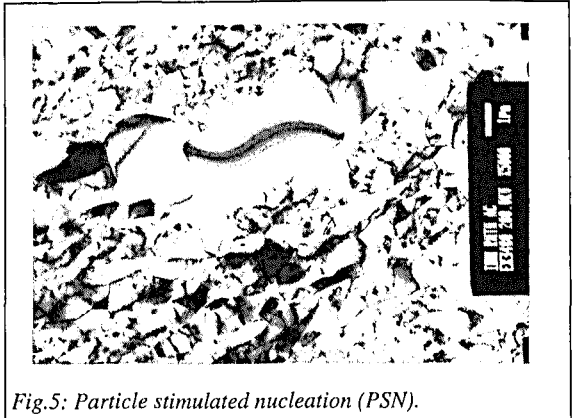


Fig.5: Particle stimulated nucleation (PSN).

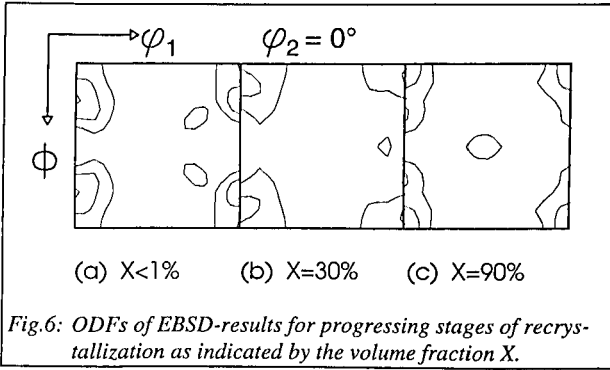


Fig.6: ODFs of EBSD-results for progressing stages of recrystallization as indicated by the volume fraction X .

Cube-grains with strong scatter around RD and TD had developed, as also confirmed by TEM-investigations (Fig.4). With progressing recrystallization this scatter diminished (Fig.6b,c). Besides the Cube-texture a weak P-orientation $\{011\}<122>$ and a large number of randomly oriented grains appeared. The ODF of the (nearly) completely recrystallized stage (Fig.6c) showed good agreement with the corresponding macrotexture (Fig.1).

In Fig.7 the orientations of the new grains at the early stages of recrystallization of the same sample are grouped according to their nucleation sites, *i.e.* in Cube-bands or in deformation zones. It is apparent that the grains from the band-like structures show Cube-orientations scattered around TD and particularly around RD (Fig.7a). This texture type is similar to the ODFs of the completely recrystallized specimens (Fig.1), even the texture sharpness is comparable.

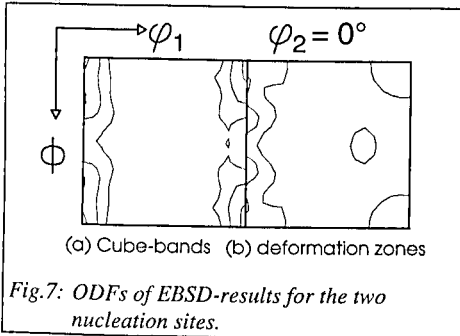


Fig.7: ODFs of EBSD-results for the two nucleation sites.

The orientations of grains from deformation zones (Fig.7b) were not totally random but surprisingly similar to those in Cube-bands (Fig.7a). However, in contrast to the Cube-bands some scatter of Cube about ND was obvious. The total intensity of the microtexture was lower, indicating a higher amount of randomly oriented grains, and additionally, some P-oriented grains had formed in the deformation zones.

Discussion

As outlined in the preceding section, in the investigated Al-Mn samples two principal sets of orientations form, which are correlated to their respective nucleation sites: (i) A strong Cube-orientation with far reaching scatter about RD and eventually also about TD. This texture type could be associated with the Cube-bands. (ii) PSN gives rise to a large amount of more or less random orientations with small maxima at the P-orientation but also a Cube-orientation with a characteristic scatter about ND. In the following the development of these two orientation groups will be discussed with respect to differences in nucleation and subsequent growth behaviour.

Formation of the Cube-texture

The formation of a strong Cube-texture has been subject of a lot of controversial discussions in literature (cf. [10,11]) and, therefore, shall only briefly be addressed here. For interpretation of nucleation of Cube-oriented grains often the Dillamore/Katoh-mechanism is cited [10-13]. In this model it is assumed that nucleation of Cube-oriented recrystallized grains occurs in so called transition bands between two parts of a previous grain with an orientation that tends to split during rolling. According to Taylor deformation models such structures can comprise the Cube-orientation as well as its scatter about RD and TD. However, it is not clear whether the spatial nucleus density in transition bands is sufficient to explain the occurrence of a strong Cube-texture. Additionally, however, the Cube-orientation may originate from former deformed grains, which retain their original orientation close to Cube [11,14,15]. As Cube-oriented subgrains are furthermore capable to rapidly recover into quite large subgrains [13], they offer excellent conditions for successful nucleation events.

In the current investigation in the Cube-bands orientations close to Cube but with strong rotations either about RD or, less pronounced, about TD were determined. The resemblance of the local texture of the subgrains in the Cube-bands (Fig.3) and of the first grains growing outside the bands (Fig.4) clearly proves a nucleation preference of these orientations.

In order to study the growth behaviour of the Cube-grains, the individual orientations of a large number of the Cube-grains were determined at various stages of recrystallization, as described above (Fig.6). At the beginning, in most cases a Cube orientation rotated either about TD or in most cases about RD was found rather than the exact Cube-orientation (*i.e.* at $0^\circ, 0^\circ, 0^\circ$) (Fig.6a). At later stages of recrystallization (Fig.6b,c) and in the macrotexture of the completely recrystallized state (Fig.1), however, the position of Cube-peak had shifted to its exact position, and only minor RD- and TD-scatter remained.

This orientation shift (Fig.4) can only be accounted for by growth selection of the exactly Cube-oriented grains stemming from the scattered spectrum of nuclei orientations. Due to the high symmetry of the exact Cube-orientation such grains have favourable growth conditions into all symmetrically equivalent components of the deformation texture between C- and S-orientation along the β -fibre. Therefore, in the long run the perfectly Cube-oriented grains grow faster than the scattered ones and generate a so called compromise texture [11].

Furthermore, the development of the grain sizes was examined separately for Cube-grains and non-Cube-grains (misoriented more than 15°) with progressing recrystallization. The results yield a distinct growth advantage of the Cube-oriented grains in comparison to other grains (Fig.8).

In conclusion, the formation of nuclei with Cube-orientation is explained by preferred nucleation in band-like structures. Owing to their formation mechanisms strong scatter about RD and - less pronounced - about TD prevails. During further growth a selection of grains with an exact Cube-orientation rather than a scattered one occurs which is attributed to compromise effects.

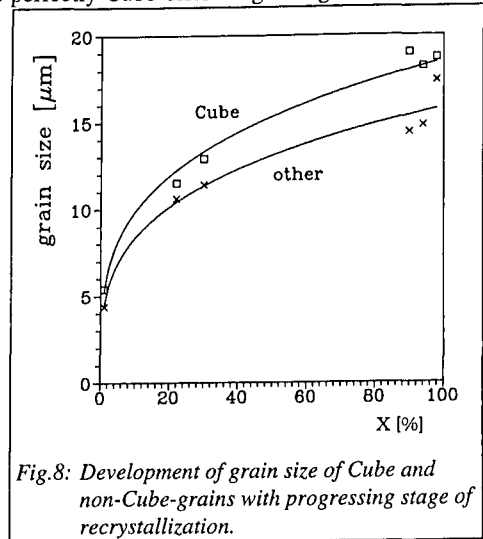


Fig.8: Development of grain size of Cube and non-Cube-grains with progressing stage of recrystallization.

Particle stimulated nucleation (PSN)

In materials containing large precipitates ($>1\mu\text{m}$) recrystallization can occur much easier than in homogeneous samples because of particle stimulated nucleation in the deformation zones around the particles [16]. During annealing one or a few of the subgrains in the deformation zones start to grow into the surrounding deformed matrix (Fig.5). Concerning the orientations of the subgrains within the deformation zones, and consequently of the potential nuclei, $\langle 112 \rangle$ -rotations of the matrix-orientations were found in single crystal experiments, which could be related to the active slip systems [16-18]. In polycrystals the rotations within the individual deformation zones can be related to the operating slip systems in a similar manner [19-21]. However, globally in a first approximation a more or less random distribution of nucleus orientations can be assumed, which is caused by the multitude of strongly scattered subgrain orientations within the deformation zones [2,3,21].

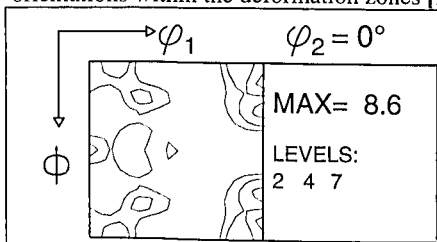


Fig.9: ODF of CBED-results in the deformation zones.

The decisive step of nucleation, which finally determines the recrystallization texture, consists of growth of a large subgrain out of the deformation zone into the surrounding deformed matrix. The orientations of 50 new grains, which obviously had nucleated from the deformation zones were determined by CBED. From the data a Gauss-ODF was calculated, the corresponding $\phi_2=0^\circ$ -section is shown in Fig.9. However, the number of measurements was definitely too small for quantitative evaluation of the results.

In this diagram remarkable intensities of the ND-rotated Cube-orientation prevail, which is in good (qualitative) agreement with the corresponding EBSD-results (Fig.7b). So it can be concluded that this texture evolution is caused already at incipient stages of recrystallization by growth selection out of the large spectrum of more or less randomly oriented nuclei around the particles (microscale growth selection). Therefore, in comparison to the microtexture from grains stemming from Cube-bands (Fig.7a) surprisingly small differences were obtained, though the original spectrum of potential nucleus orientations is substantially different.

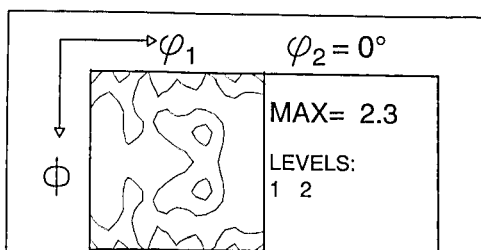


Fig.10: $40^\circ \langle 111 \rangle$ -transformed rolling texture (92% red.).

In order to access the contribution of growth selection to the final recrystallization textures more quantitatively, an arithmetical transformation of the rolling texture by $\pm 40^\circ$ around all possible $\langle 111 \rangle$ -axes was performed. As an example, in Fig.10 the $\phi_2=0^\circ$ -section of the resulting so called "transformed rolling texture" is presented. By comparing the position of the resulting peaks (Fig.10) with the microtexture of grains nucleated in the deformation zones (Figs. 7b,9) a strong resemblance becomes evident. The ND-scattered Cube- as well as the P-orientation are reproduced, also the intensities of these orientations are comparable.

However, the comparison between the transformed rolling texture (Fig.10) and the macrotexture after complete recrystallization (Fig.1) also reveals specific differences, which in particular pertain to the Cube-orientation. As the Cube-oriented grains were attributed to nucleation at the Cube-bands (see above), it can be concluded that a competition occurs between grains nucleating by PSN and those nucleating at Cube-bands, which finally determines the recrystallization texture, as discussed in more detail in Ref. [6].

Interaction of deformation zones and Cube-bands

The deformation zones around the large Al_6Mn -precipitates and the Cube-bands can interact, as *e.g.* apparent from Fig.11. The precipitates are often located at the grain boundaries between prior grains. Additionally, it was reported that large particles even can give rise to the formation of fine band-like structures as *e.g.* transition bands [21,22]. Although the underlying mechanisms are not yet clear, it is easy to imagine that orientation splitting, which is a precursor to the formation of transition bands, is initiated near the particles. In such cases the particles exert only a "catalytic effect" [22] without directly interfering with the recrystallization texture development. However, since the respective volumes of deformation zones and Cube-bands can overlap, it is difficult to decide by EBSD-measurements in the SEM, whether a new grain stems from a deformation zone or from a Cube-band. Consequently, the Cube-orientation in the ODF of the microtexture of the deformation zones (Fig.7b), which was attributed to PSN, might be overestimated.

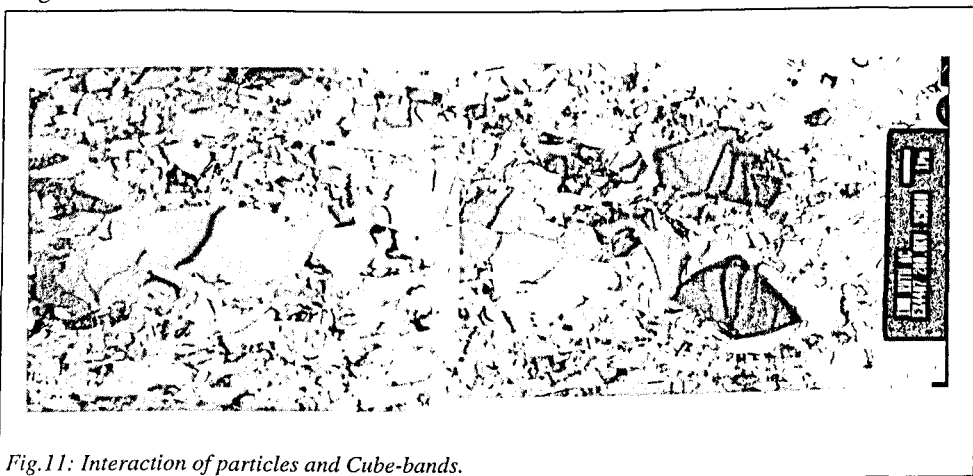


Fig.11: Interaction of particles and Cube-bands.

Conclusions

In the current investigation the formation of recrystallization textures of binary Al-1.3%Mn alloys containing large (2-3 μ m) Al_6Mn -precipitates was studied with respect to the nucleation and growth behaviour of the various components of the deformation structure. Different mutually complementary techniques were employed to elucidate recrystallization mechanisms on a micro-, meso- and macroscale. The following conclusions can be drawn:

- The formation of the recrystallization texture can be explained by a competition between grains nucleating in Cube-bands and grains from particle stimulated nucleation (PSN).

- o The development of the Cube-texture in the used material is very similar to that obtained in high purity Al. Grains with Cube- and particularly with slightly rotated Cube-orientations nucleate in band-like structures, which are already present in the deformed microstructure (either transition bands or deformed grains with retained Cube-orientation). During the subsequent growth, however, grains with an exact Cube-orientation prevail due to their optimum growth conditions into several deformation components (compromise effect).
- o Particle stimulated nucleation ("PSN") occurs in the deformation zones around the Al₆Mn-precipitates. Starting from a (globally) more or less random spectrum of subgrain orientations in the deformation zones only those nuclei with a preferred orientation relationship grow out of the deformation zones into the deformed matrix. This results in rather random orientations with some preference of the P-orientation and a characteristic scatter of Cube about ND.

References

1. D. Juul Jensen, N. Hansen, F.J. Humphreys, *Acta metall.* **33**, 2155 (1985).
2. R. Ørsund, E. Nes, *Scripta metall.* **22**, 665, 671 (1988).
3. A. Oscarsson, *Textures and Microstructures* **14-18**, 477 (1991)
4. T. Rickert, S. Guldborg, T. Furu, E. Nes, K. Lücke, *Textures and Microstructures* **14-18**, 721 (1991).
5. K. Lücke, O. Engler, in *Proc. 3rd Int. Conf. on Al-Alloys (ICAA 3)*, (eds. L. Arnberg et al.), the Norwegian Inst. of Tech., Trondheim, Vol.III, 439 (1992).
6. O. Engler, P. Yang, X.W. Kong, submitted to *Acta metall. mater.* (1994)
7. H.J. Bunge, *Mathematische Methoden der Texturanalyse* Akademie, Berlin (1969).
8. K. Lücke, J. Pospiech, J. Jura, J. Hirsch, *Z. Metallk.* **77**, 312 (1986).
9. O. Engler, G. Gottstein, *steel research* **63**, 413 (1992).
10. J. Hjelen, R. Ørsund, E. Nes, *Acta metall. mater.* **39**, 1377 (1991).
11. J. Hirsch, in *Proc. 7th Risø Int. Symp.* (eds. N. Hansen et al.), Risø Nat. Lab., Roskilde, 349, 361 (1986); and in *Habilitation Thesis* RWTH Aachen (1988).
12. I.L. Dillamore, H. Katoh, *Metal Sci.* **8**, 73 (1974).
13. A.L. Dons, E. Nes, *Mat. Sci. Tech.* **2**, 8 (1986).
14. H. Weiland, J.R. Hirsch, *Textures and Microstructures* **14-18**, 647 (1991).
15. O. Daaland, C. Maurice, J. Driver, G.-M. Raynaud, P. Lequeu, J. Strid, E. Nes, in *Proc. ICAA 3*, as Ref. [5], Vol.II, 297 (1992).
16. F.J. Humphreys, *Acta metall.* **25**, 1323 (1977).
17. K.C. Russell, M.F. Ashby, *Acta metall.* **18**, 891 (1970).
18. O. Engler, J. Hirsch, K. Lücke, in *Proc. ICOTOM 8*, (eds. J.S. Kallend, G. Gottstein), TMS Warrendale 637 (1988).
19. X.W. Kong, O. Engler, K. Lücke, *Textures and Microstructures* **14-18**, 1215 (1991); and in preparation.
20. F.J. Humphreys, P.N. Kalu, *Acta metall. mater.* **38**, 917 (1990).
21. F. Habiby, F.J. Humphreys, *Textures and Microstructures* **20**, 125 (1993).
22. E. Nes, in *Proc. 1st Risø Int. Symp.* (eds. N. Hansen et al.), Risø Nat. Lab., Roskilde, 85 (1980).